HHS Public Access

Author manuscript

J Immunol. Author manuscript; available in PMC 2017 September 15.

Published in final edited form as:

J Immunol. 2016 September 15; 197(6): 2509–2521. doi:10.4049/jimmunol.1502659.

Immunotherapy expands and maintains the function of high affinity tumor infiltrating CD8 T cells in situ

Amy E. Moran, **Fanny Polesso**, and **Andrew D. Weinberg**

Earle A Chiles Research Institute, Robert W. Franz Cancer Research Center, Portland Providence Medical Center, 4805 NE Glisan Ave, 2N35, Portland, OR 97213

Abstract

Cancer cells harbor high affinity tumor-associated antigens capable of eliciting potent anti-tumor T cell responses yet detecting these polyclonal T cells is challenging. Therefore, surrogate markers of T cell activation such as CD69, CD44, and PD-1 have been used. We report here that in mice, expression of activation markers including PD-1 is insufficient in the tumor microenvironment to identify tumor-antigen specific T cells. Using the Nur77GFP T cell affinity reporter mouse, we highlight that PD-1 expression can be induced independent of TCR ligation within the tumor. Given this, we characterized the utility of the Nur77GFP model system in elucidating mechanisms of action of immunotherapies independent of PD-1 expression. Co-expression of Nur77GFP and OX40 identifies a polyclonal population of high affinity tumor-associated antigen-specific CD8+ T cells, which produce more IFNγ *in situ* than OX40 negative and doubles in quantity with anti-OX40 and anti-CTLA4 mAb therapy but not with anti-PD-1 or PD-L1. Moreover, expansion of these high affinity CD8 T cells prolongs survival of tumor bearing animals. Upon chronic stimulation in tumors and after adoptive cell therapy, CD8 TCR signaling and Nur77GFP induction is impaired and tumors progress. However, this can be reversed and overall survival significantly enhanced after adoptive cell therapy with agonist OX40 immunotherapy. Therefore, we propose that OX40 agonist immunotherapy can maintain functional TCR signaling of chronically stimulated tumor resident CD8 T cells thereby increasing the frequency of cytolytic, high affinity, tumor-associated antigen-specific cells.

Introduction

The ability to mediate rejection of a tumor relies on both the quantity and the quality of the responding immune cell infiltrates. In particular, CD8+ T cell anti-tumor immune responses can be highly cytolytic leading to tumor destruction, generation of lasting T cell memory, and ultimately tumor-free survival. However, the antigen sensitivity and specificity of CD8+ T cells is tightly regulated and the ability of tumor antigens to evoke a potent, cytolytic T cell response is still under investigation. Given that many tumor-associated antigens are overexpressed self-antigens, the T cell receptor repertoire reactivity to these antigens can be weak and curtailed resulting in the production of dysfunctional T cells and poor anti-tumor immune responses (1). However, work from multiple groups provides evidence that within

Correspondence should be addressed to: Amy Moran, 4805 NE Glisan Ave. 2N-C29, Portland, OR, 97213, Phone: 503-215-3975 Fax: 503-215-6841 amy.moran@providence.org.

tumors there are novel antigens that are non-overlapping from the normal genome termed neoantigens (2). These mutated proteins, arising from tumor-specific DNA instability, promote the generation of neoantigens, some of which contain high affinity peptides capable of eliciting cytolytic and sustained anti-tumor T cell responses (3–6). Theoretically, these neoantigens serve as tumor rejection antigens for which lymphocyte-mediated immune responses can be modified with immune based cancer therapies (7, 8). Moreover, these neoantigens may serve as important biomarkers for predicting the efficacy of immunotherapy and/or for the generation of tumor-antigen specific T cell therapies in patients with solid tumors(9–11). However, identifying and measuring the strength of TCR signals to these unknown tumor antigens remains challenging.

Historically, in the absence of known tumor antigens, TCR transgenic (Tg) mice were employed to study T cell tumor-antigen specific immune responses. These experiments relied on the expression of a tumor-associated antigen (often a foreign or model tumor antigen such as ovalbumin) by the tumor cells and for which a known TCR Tg line was available. While these initial studies provided a robust foundation for our understanding of T cell-tumor cell interactions, some have argued that they do not reflect the natural affinity of endogenous TCRs for tumor associated antigens (12). Therefore, others have utilized traditional markers of antigen encounter such as CD69, CD44, and PD-1 to identify tumor antigen specific T cell responses when the antigen specificity of the T cells is unknown (13, 14). Implicit in these observations is that there are activating tumor-associated antigens in the tumor. However, even in the presence of these seemingly ‘antigen specific’ T cells, tumors progress (12, 15). Therefore, the mere presence of CD69+ or PD-1+ T cells within the tumor may not be indicative of an ongoing antigen-specific response. In fact, in models of acute infection and inflammation, inflammatory cytokines such as type I interferon can also mediate the up regulation of CD69 and CD44 (16–18). However, the idea that CD69, CD44, and PD-1 can be induced in a similar bystander manner within the tumor has not been addressed.

There is mounting evidence that tumor-associated antigens can serve as tumor rejection antigens and induce T cells that are highly cytolytic and mediate tumor regression (3, 4). These experiments utilize techniques that identify mutated genes or altered self-proteins expressed by the tumor, which bind self MHC. Investigators have been able to track endogenous T cells specific for these antigens. But what about tumor models in which the antigens are undetermined and the TCR specificity of the tumor-infiltrating lymphocytes are unknown? How does one study the reactivity of T cells to tumor-associated antigens in these models and the affinity of the TCR response? To address these questions, we took advantage of a recently characterized experimental tool. The orphan nuclear receptor Nur77 (Nr4a1) is an immediate early gene rapidly up-regulated in response to antigen receptor signaling *in vitro* and *in vivo* (19, 20). Two independent groups reported the generation bacterial artificial chromosome transgenic (BAC Tg) mice in which GFP expression is under the control of the Nr4a1 transcriptional elements (21, 22). Using altered peptide ligands ranging from very low affinities (non-activating) to very high affinity (deletion) for the OT-I TCR Tg mouse, it was shown that this Nur77GFP model faithfully reported a range of TCR affinities in CD4 and CD8 T cells and unlike CD69, the upregulation of Nur77GFP was TCR ligation-dependent

(and independent of inflammation or IL-2) consistent with Nur77 being a TCR immediate early gene and NFAT regulated molecule (21, 22).

Interestingly, these endogenous T cells with high affinity antigen receptors also express co-stimulatory molecules. One of these molecules, OX40, first described on activated rat lymphocytes (23), is a tumor necrosis family receptor member (TNFR) expressed primarily on activated CD4 and CD8 T cells in both mouse and humans. Foxp3+ CD4 regulatory T cells (Tregs) in mice constitutively express OX40 while in humans, Tregs express low levels of OX40 in the blood but OX40 expression is induced within inflammatory lesions such as the tumor in 20–60% of Foxp3+ T cells (24). Co-stimulation through OX40 is reported to promote T cell division, survival, and restore the cytolytic function of anergic cells (25–27). In addition, treatment of tumor-bearing mice with an agonist OX40 monoclonal antibody (mAb) leads to a 20–80% cure rate in multiple tumor models (25). In a phase I study of patients with a variety of cancers, three doses of an anti-OX40 agonist mAb increased proliferation and IFNγ production of CD8 T cells in these patients, and importantly, led to tumor shrinkage of at least one tumor nodule in 40% of patients treated (28).

We tested the hypothesis that utilization of the TCR affinity reporter system in Nur77GFP mice would facilitate identification of CD8 T cells receiving strong TCR signals from cells presenting tumor-associated antigens in the context of MHC and provide a tool by which we could interrogate antigen-specific T cell responses and investigate the mechanism of action of anti-OX40 agonist mAb immunotherapy. We illustrate that Nur77GFP (herein referred to as GFP) upregulation is a more faithful marker of tumor-antigen specific T cell responses than traditional markers of T cell activation including PD-1. We highlight that CD8 T cells can up-regulate PD-1 within the tumor independent of TCR ligation, which suggests bystander induction. Moreover, we demonstrate that within the first 5 days after tumor inoculation there is an enrichment of GFPhi T cells in the draining lymph node as compared to the tumor consistent with the activation of high affinity tumor-antigen specific T cells. However, once the tumors are well established, this ratio flips and there is an increase in GFPhi T cells in the tumor as compared to the draining lymph node. In addition, these tumor residing CD8 T cells make more IFNγ than GFPlow T cells, and are selectively expanded by OX40 agonist and anti-CTLA4 immunotherapy. In addition, we reveal a means by which the kinetics of strong TCR responses to tumor antigens after immunotherapy can be studied. Using the OT-I TCR Tg model system, we establish that the Nur77GFP reporter system can be used to identify novel mechanisms of action of immunotherapy agents in regards to maintaining TCR-mediated GFP upregulation. Together, these data provide evidence that a mechanism of action of agonist anti-OX40 mAb immunotherapy resides in its ability to promote and sustain high affinity anti-tumor T cell responses within the endogenous T cell repertoire or after adoptive cell therapy.

Materials and Methods

Animal and tumor models

Nur77GFP mice were provided by K.A. Hogquist (University of Minnesota, Minneapolis, MN), were maintained as heterozygous transgene carries, and were bred to either B6, 129, or Foxp3RFP animals purchased from The Jackson Laboratory. Male and female animals

were used for the MCA205 studies presented. Male animals were used for TRAMPC-1 and d42m1-T3 tumor studies. OT-I;Thy1.1 TCR transgenic, and OVA-tolerant transgenic mice in which the prostate specific probasin promoter was used to control expression of membrane OVA (referred to as POET-1) (29) were bred and maintained under specific pathogen-free conditions in the Providence Portland Medical Center (Portland, OR) animal facility. Both male and female OTI;Thy1.1;Nur77GFP animals were used in adoptive transfer experiments. Female POET mice were used for MCA205OVA experiments. Wild-type C57BL/6 mice were purchased from The Jackson Laboratory. All animal experimentation was approved by and performed according to guidelines from the Institutional Animal Care and Use Committee at the Providence Portland Medical Center. Murine MCA205 H12 sarcoma cells (gift of Suyu Shu), B16 melanoma cells and 3LL/Lewis lung carcinoma cells (purchased from ATCC) were propagated *in vitro* using Complete Media, RPMI (Lonza) containing .292ng/mL glutamine, 100U/ml streptomycin and penicillin, nonessential amino acids, 1mmol/L sodium pyruvate and 10mmol/L HEPES (Sigma). D42m1-T3 tumor cells were generously provided by Robert Schreiber and were cultured in the above culture media supplemented with 0.1% 2-mercaptoethanol. All cell lines were tested and confirmed to be *Mycoplasma* and endotoxin-free using the MycoAlert Detection Kit (Lonza) and the Endosafe-PTS sytem (Charles River Laboratories). All culture media reagents were purchased from Hyclone Laboratories unless noted. Control rat IgG antibody was purchased from Sigma whereas rat anti-OX40 antibody (OX86), rat anti-CTLA4 (9D10) and anti-PD-1 (G4; a gift from Dr. C. Drake, John Hopkins University) mAbs were produced in the laboratory from hybridomas and affinity purified over protein G columns. Anti-PD-L1 (10F. 9G2) purified mAb was purchased from BioXCell. Animals were randomly assigned to treatment cohorts and tumors were ~70mm^2 (by 2-dimension caliper measurement) at the start of treatment unless indicated otherwise. Any animal with a tumor larger than 200mm^2 was euthanized per our guidelines from the Institutional Animal Care and Use Committee and these animals were not included in the experiment. No outliers were excluded from the data presented.

Lymphocyte isolation and analysis

Tumor draining lymph nodes (dLN) (inguinal) and spleens were harvested and processed to obtain single-cell suspensions using frosted ends of microscope slides. Spleens were incubated with ammonium chloride potassium (30) lysing buffer (Lonza) for 3 minutes at room temperature to lyse red blood cells. Cells were then rinsed with PBS containing 1% FBS and 4mM EDTA. For flow cytometry analysis, cells were incubated for 20 minutes on ice with fixable viability dye, TCRβ (H57–597), (RM4–5), CD8 (53–6.7), CD3 (17A2), CD69 (H1.2F3), CD44 (IM7), PD-1 (J43), OX40 (OX86), Thy1.1 (H1S51), Vα2 (B20.1), or Vβ5 (MR9-4). All antibodies and viability dyes were obtained from eBioscience or BioLegend. MHC class I tetramers were generated by the NIH Tetramer Facility for assessing H-2D^b:Spas1 (peptide sequence STHVNHLHC), H-2K^b:mLama4 (peptide sequence VGFNFRTL), H-2K^b:OVAp (peptide sequence SIINFEKL) specific T cell responses in TRAMPC-1, d42m1-T3, and MCA205OVA tumors, respectively. Unless noted otherwise in the figure legend, cells were gated through live/TCRβ+/CD8+ gates for analysis. Intracellular proteins (IFNγ and Ki67) were detected using the Foxp3

Transcription Factor Concentrate and Diluent from eBioscience. Cells were analyzed with an LSR II flow cytometer (BD Biosciences) using FlowJo software (Tree Star).

In situ cytokine production

For *in situ* cytokine detection in tumor infiltrating CD8 T cells we used a protocol previously developed by Whitton's group (31). Briefly, animals were injected intravenously with 0.25 mg of brefeldin A (BFA) (Life Technologies) 5 hours before animals were euthanized and lymphocytes isolated. All tissues were immediately placed in ice cold PBS+1% FCS containing 10mg/mL BFA. BFA remained in staining buffer and through fixation and permeabilization of the cells.

In vitro activation and intra-cellular cytokine staining

Splenocytes and tumor infiltrating lymphocytes (TIL) were plated at 10^6 cells per well in 96-well plates and stimulated for 5 hours with 5μg/mL anti-CD3 mAb (145-2C11) or PMA (80nM)/ionomycin (1.3μM), in the presence of BFA. Cells were then stained for surface markers, fixed and permeabilized and stained for intracellular cytokines.

Tumor challenge and tumor immune infiltrate isolation

A total of 0.5×10^6 MCA205, 1×10^6 MCA205-OVA, 0.1×10^6 B16, 1×10^6 TRAMP-C1 (TC1), 1×10^6 3 Lewis Lung (3LL), or 1×10^6 d42m1-T3 murine tumor cells were injected subcutaneously into the right and/or left flank of Nur77GFP, POET-1, C57BL/6, or Nur77GFP;129 F1 mice (day 0). MCA205 and MCA205-OVA tumor bearing mice received rat immunoglobulin G (rat IgG; up to 2 × 250μg; Sigma), anti-OX40 (up to 2 × 250μg, clone OX86), anti-CTLA4 (2 × 250μg; clone 9H10), anti-PD-1 (3 × 200μg; clone G4; provided by Dr. C. Drake, John Hopkins University), or anti-PD-L1 (3 × 200μg; clone 10F.9G4; BioXCell). All mAbs were verified to be endotoxin-free and injected intraperitoneally (i.p.) into recipient mice. Tumor growth (area) was monitored with microcalipers and treatments began when tumors were approximately $70mm^2$ (~10 days after injection) and animals were sacrificed when tumors reached $200mm^2$ or according to treatment timeline, as described. Tumor infiltrating lymphocytes (TIL) were harvested by dissection of tumor tissue into small fragments in a 50cc conical tube followed by digestion at room temperature in a bacterial shaker for 30 minutes in 1mg/mL collagenase type IV (Worthington), 100μg/mL hyaluronidase (Sigma), and 20mg/mL DNAse (Roche) in PBS. Following filtration and further cell disruption with a 1cc syringe plunger through a 70 micron nylon cell strainer (BD), tumor cells, splenocytes, and lymphocytes were stained.

Adoptive transfer

Single-cell suspensions were prepared from the spleens of OT-I Thy1.1 TCR transgenic mice. ~$10–20 \times 10^6$ bulk splenocytes (which consistently contained ~12.5% OT-I T cells or ~$1.25–2.5 \times 10^6$ OT-I T cells) were injected i.v. (day 0) in 200μL of PBS into POET-1 MCA205 or MCA205-OVA tumor bearing mice when the tumors reached ~$75mm^2$. Animals were treated with 250 μg anti-OX40 (clone OX86) or 250 μg control rat IgG (day 1 and day 5). Alternatively, 8×10^6 bulk splenocytes (containing 1×10^6 OT-I T cells) were injected

i.v. into Nur77GFP MCA205 or MCA205-OVA tumor bearing mice. Animals were euthanized, tumors harvested, TIL extracted and analyzed on indicated days.

Statistical Analysis

Statistical analysis was performed using unpaired two-tailed Student's *t* test (for comparisons between 2 groups), one-way ANOVA for multiple comparisons, or the Mantel-Cox method (log-rank test) for survival analysis using GraphPad Prism 6 (GraphPad Software Inc.). Error bars represent SEM unless noted otherwise in the figure legend. Statistical tests and *P* values are specified for each panel in the respective figure legends and *P* values of <0.05 were considered significant. Biological replicates (individual animals) for each experiment are indicated as *n* in the figure legends.

Results

Markers of T cell activation can be misleading in the tumor

The tumor microenvironment is rich in inflammatory factors such as vascular endothelial growth factor, prostaglandin E2, IL-10, and type I interferons (32, 33). Some of these factors can induce markers of T cell activation, independent of TCR ligation (16, 17). This can be problematic when attempting to segregate true CD8 T cell responses to a specific tumor-associated antigen from cognate-antigen independent bystander inflammation in the polyclonal setting. Therefore, we assessed whether a TCR affinity reporter mouse could be used to distinguish inflammatory from TCR-specific signals in the tumor microenvironment. To this end, we inoculated Nur77GFP mice with melanoma, lung carcinoma, or methylcholanthrene-induced sarcoma tumor cell lines. Tumors were harvested when they reached ~80–100mm^2 and we analyzed CD69, CD44, and PD-1 on CD8 T cells in the tumor and dLNs. In the dLN, only a small fraction of CD8 T cells exhibited increased expression of CD69 and CD44, and nearly all cells were PD-1 low (Fig. 1A, shaded histogram). In the MCA205 and 3LL tumors however, nearly all of the CD8 TIL were CD69 and CD44hi and in all three-tumor models, PD-1 expression was enriched on all tumor isolated CD8 T cells. CD69 is a transient marker of T cell activation in that it is rapidly (within 12 hours) up-regulated after TCR engagement following antigen encounter (34) but then returns to baseline approximately 48 hours later. CD69 also antagonizes the sphingosine-1-phosphate receptor to retain effector and memory T cells in peripheral tissues (16, 30). In contrast, CD44 expression requires approximately 24–48 hours for maximal expression after TCR engagement and then remains high as a result of antigenic stimulation (35). Therefore, we thought co-expression of CD69 and CD44 might identify a population of CD8 T cells that were actively encountering their cognate ligand in the tumor. However, given that the majority of CD8 T cells co-expressed CD69 and CD44 in the MCA205 and 3LL tumors (Figure 1A), we could not use these markers to distinguish a sub-population of tumor-reactive T cells. Therefore, we turned to the Nur77GFP model to determine if it accurately delineated a tumor-reactive population of CD8 T cells. Using this GFP reporter system, we observed significant differences in the expression of GFP when compared to CD69, CD44, or PD-1 on CD8 TIL (Figure 1B). In all 3 tumor lines, the majority of the CD8 T cells were GFPlo; only a small fraction of T cells expressed high levels of the GFP reporter. Taken together, this suggests that CD44, CD69, and PD-1 expression do not reliably identify T

cells that have recently undergone TCR ligation and antigen encounter within the tumor microenvironment.

Of interest to our studies was whether or not we could identify a population of T cells within the tumor that were receiving strong TCR signals at the time of harvest. Because the half-life of Nur77-induced GFP is approximately 55 hours *in vivo* and begins to decay upon pMHC:TCR dissociation (22), we felt the Nur77GFP model system was ideal for detecting T cells receiving strong TCR signals at or just before the time of harvest. When we compared the frequency of CD8+GFPhi T cells in the tumor versus the spleen of the same tumor-bearing mouse, we observed a 2.9-fold increase in GFPhi T cells in these well-established tumors (Figure 1C bar graph). These T cells were enriched for PD-1 expression, although not all were PD-1+ (Figure 3A), suggesting the presence of a population of tumor-associated antigen specific T cells receiving strong TCR signals. Collectively, these results suggest that while CD44, CD69, and PD-1 can often be co-expressed in the tumor microenvironment, the Nur77GFP TCR reporter has a distinct expression pattern.

Antigen encounter regulates Nur77GFP upregulation within the tumor

Given the enrichment of GFPhi CD8 T cells in the tumor, we sought to determine if GFP up-regulation faithfully reported TCR engagement in the tumor microenvironment or could also be induced in a bystander fashion. We utilized K^b/OVA-specific OT-I T cells and OVA as a model tumor antigen. Splenocytes from OT-I/Thy1.1/Nur77GFP mice were adoptively transferred into OVA tolerant mice (POET-1) bearing either established MCA205 (wild-type or WT) or MCA205-OVA (OVA) expressing tumors. Five days following adoptive transfer, OT-I T cells were isolated from the spleen and tumor of tumor-bearing animals. The frequency of OT-I T cells was significantly higher in the OVA-expressing tumors with a small but detectable population of OT-I T cells in the non-OVA expressing tumors (Figure 2A). Consistent with the presence of cognate antigen in the OVA+ tumor, these OT-I T cells also expressed lower levels of TCR Vα2 (Figure 2A), and were PD-1hi, CD44hi, and CD69hi in the OVA bearing tumors (Figure 2B, solid lines). Similar to what was observed in the polyclonal environment and has been reported for T cells isolated under inflammatory conditions (17), OT-I T cells from the WT tumor also expressed high levels of CD69 and CD44 (Figure 2B, dotted line). Surprisingly, PD-1 expression was nearly identical on OT-I T cells in OVA expressing or WT tumors suggesting that factors in the tumor microenvironment other than TCR engagement could mediate PD-1 up-regulation of antigen inexperienced T cells. There was a 3–6 fold enrichment in GFP MFI (Figure 2B, far right) in the OT-I Nur77GFP T cells isolated from OVA-antigen bearing tumors when compared to WT tumors. Together, this suggests that TCR ligation and not T cell extrinsic factors within the tumor microenvironment regulate Nur77-derived GFP induction.

Endogenous tumor-antigen specific CD8 T cells can be Nur77GFP^{hi}

There is mounting evidence that some cancer neo-epitopes are capable of eliciting potent anti-tumor immune responses (7, 8, 10, 11). These immunogenic neoantigens result in stable peptides in MHC molecules and their subsequent affinity for their cognate TCR are hypothesized to be very strong (2, 3). With this in mind, we took advantage of the OT-I/K^b:OVAp transgenic system that gives a robust GFP signal (22, 36) and is known to be a

high affinity interaction. Using this as a 'yardstick' to establish the highest affinity T cell response we would expect to observe *in vivo*, we inoculated Nur77GFP mice with MCA205OVA-expressing tumors and once the tumors were established, adoptively transferred congenically labeled OT-I/Nur77GFP T cells. Six days after adoptive transfer, we isolated the transferred T cells and compared the mean GFP fluorescent intensity (MFI) of OT-I T cells to the endogenous CD8 TIL. Interestingly, the OT-I T cell GFP MFI significantly overlapped with the GFP MFI of the top ~8% of polyclonal CD8 T cells in the same tumor (Figure 3A) and the GFP brightest CD8 T cells expressed intermediate levels of PD-1. Given that maximum GFP induction (6–12hrs post TCR ligation) precedes PD-1 induction (12–24hrs), it is possible that these GFP-brightest PD-1 intermediate T cells are those that most recently encountered their cognate ligand within the tumor.

Next, we sought to assess TCR signal strength of endogenous T cell responses to an array of tumor-associated antigens. We choose two model neoantigens generated from point mutations in the native peptides in the 'stimulate prostatic adenocarcinoma specific T cell' SPAS-1 epitope from TRAMPC-1 tumors and the mutant laminin alpha subunit 4 (mLama4) epitope from the d42m1-T3 sarcoma. In addition, we also assessed the endogenous TCR affinity to the model tumor antigen ovalbumin (OVAp). The SPAS-1 mutated peptide was shown to protect ~30% of mice prophylactically treated with the mutated peptide (37). In contrast, when the mLama4 peptide and a second peptide (mAlga8) was provided in a prophylactic setting, ~80% of d42m1-T3 animals rejected their tumors (3). In all three tumor models, we could detect endogenous tumor-antigen specific CD8 T cells using MHCI tetramers and the frequency of tetramer + T cells varied between tumors (Figure 3B). Of note, only a fraction of endogenous tetramer positive T cells were GFPhi. However, each tumor contained tetramer positive T cells with overlapping GFP levels (compare Figure 3B tetramer positive fractions) in any of the tumor models assessed consistent with each of these neo-antigens capable of promoting tumor rejection. In the TRAMPC-1 tumors, ~10% of the total population was GFPhi where as in the d42m1-T3 model ~40% were GFPhi and almost 75% of the OVAp tetramer positive cells in the MCAOVA model were GFPhi 5–7 days after tumor implantation. The low frequency of tetramer positive GFPhi T cells in the d42m1-T3 and TrampC1 tumors could reflect differences in the tumor microenvironment and availability/accessibility of pMHC complexes for TCR recognition, antigen loss within the tumor, or the vascularity of the tumor with contaminating tetramer positive T cells residing in the blood rather than the tumor where antigen is present. In contrast to this observation, all tetramer positive cells were PD1 intermediate or hi (Figure 3B, bottom).

Given the rapid decay of GFP after pMHC:TCR disassociation (22) and the differences in the frequency of GFPhi T cells in the various tumor models above, we next asked about whether the low frequency of endogenous GFPhi CD8 T cells reflected limited tumor antigen exposure and/or an inability to upregulate Nur77GFP after antigen encounter. Others have shown that anti-CD3 stimulation of Nur77GFP expressing T cells establishes the maximum GFP signal (22, 38) *in vitro* and *in vivo*. Therefore, we harvested tumors and spleens from Nur77GFP mice and divided them into three cohorts directly ex vivo: unstimulated, anti-CD3 stimulated, or phorbol 12-myristate 13-acetat (PMA) and ionomycin stimulated. We anticipated the latter two stimuli to non-specifically induce GFP up-regulation in all T cells (Figure 3, spleen) and we could compare this to the unstimulated

control. Unexpectedly, the majority of CD8 T cells in the tumor but not the spleen were refractory to Nur77-mediated GFP upregulation after anti-CD3 stimulation (Figure 3C tumor vs spleen) but GFP upregulation was inducible by PMA and ionomycin (Figure 3C–D). Taken together, this suggests we can detect a small population of endogenous tumor infiltrating CD8 T cells that have recently received high affinity TCR signals *in situ* and have an intact NFAT mediated Nur77 upregulation signaling cascade.

T cells receiving strong TCR signals within the tumor produce IFNγ

One of the hallmarks of a CD8 T cell receiving a strong TCR signal in the presence of co-stimulation is the ability to generate effector cytokines (39) . However, assessing the *in situ* TCR signal strength and effector cytokine potential of tumor antigen reactive T cells is challenging when the tumor antigens are unknown. IFNγ production is tightly regulated by antigenic stimulus, peaking within 6 hours after antigen encounter and is shut off within 2 hours after the antigen is withdrawn (40). Interestingly, GFP induction is also tightly regulated by antigen encounter, peaking 6–12 hours after antigen receptor ligation (22). In light of the similar ‘on’ kinetics of GFP induction and IFNγ production, we hypothesized that if we could detect IFNγ producing T cells *in vivo*, we could simultaneously assess the affinity of the antigen inducing cytokine production. Because the dominant MCA205 tumor-associated antigens are unknown, we performed ‘direct ICCS’ or *in vivo* intracellular cytokine analysis (31). In the dLN of tumor-bearing animals treated with the PBS control, there is minimal detection of IFNγ *in situ* (Figure 4A). In contrast, tumor-bearing animals injected intravenously with brefeldin A (BFA) had a significant increase in the frequency of IFNγ+ CD8 T cells in the dLN suggesting that we can assess effector cytokine production *in situ* (Figure 4A).

Next, we sought to determine whether the Nur77GFPhi population of CD8 TIL was enriched for IFNγ *in situ*. We observed a significant enrichment of the Nur77GFPhi T cells in the IFNγ+ fraction as compared to the IFNγ negative population (Figure 4B). It is interesting to note, however, that not all IFNγ+ T cells are GFPhi within the tumor. In fact, ~1.5% of the IFNγ+ CD8 T cells in the tumor were GFPlow (Figure 4C), consistent with the ‘on’ kinetics of IFNγ production preceding the maximal induction of GFP by as much as 5 hours (22, 40). In addition, we observed a significant increase in the frequency and MFI of IFNγ producing CD8 T cells in the GFPhi population of TIL as compared to the GFPlow (Figure 4C & 4D). It is also important to note that our observation is probably an under estimation of the frequency of CD8 tumor antigen-specific T cells capable of making IFNγ *in situ*. To this point, when we stimulated CD8 TIL with PMA/ionomycin directly after isolating them from the tumor, we detect 17–20% of the CD8 T cells are IFNγ producers (Figure 3C top). Therefore, due to the rapid on/off kinetics of IFNγ production and Nur77GFP induction and/or decay, it is likely that there are CD8 T cells within both the Nur77GFPhi and low populations that are tumor antigen reactive but at the time of tumor harvest, had not recently encountered their cognate ligand. Intriguingly, we observed a significant enrichment (~10 fold) in the frequency of Nur77GFPhi IFNγ+ CD8 T cells in the tumor as compared to the dLN of tumor bearing mice (Figure 4C). This observation is consistent with previous studies suggesting that naïve CD8 T cells can be primed and acquire effector function within the tumor as opposed to initial activation in the lymph node and trafficking to the tumor (41).

Therefore, we propose that we can identify a population of endogenous CD8 T cells receiving high affinity TCR signals (GFPhi) from tumor-associated antigens via their ability to make IFNγ+ *in situ*.

Anti-OX40 immunotherapy increases the frequency of Nur77GFPhi TIL

Our lab has a long-standing interest in enhancing the anti-tumor immune response by targeting the TNFR family co-stimulatory molecule OX40. In mice but not humans (24), OX40 is constitutively expressed by CD4+Foxp3+ T cells (Figure 5A) and in both species, it can be induced on conventional CD4 and CD8 T cells in both an antigen dependent and independent manner (Figure 5A) (42–44). Given that OX40 is significantly up-regulated on tumor infiltrating CD8 T cells in the mouse (Figure 5A) and in human head and neck tumors (24) we asked whether the OX40 co-stimulatory protein was co-expressed on GFPhi CD8 TIL. OX40+CD8 T cells were rare in the lymph nodes of tumor-bearing animals but within the tumor, there was a significant increase in OX40 expression on all CD8 T cells (Figure 5A–B). However, the MFI of OX40 on CD8 T cells within the tumor was lower than that of regulatory T cells (Figure 5A). Next, when we compared the GFPhi population to the GFPlow population, we observed that almost 80% of the GFPhi CD8+ TIL expressed OX40 (Figure 5C) with a concurrent 1.9 fold increase in OX40 MFI of the CD8 GFPhi fraction compared to the GFPlow fraction (Figure 5C). This observation suggested that we might be able to promote the expansion of CD8 T cells receiving strong TCR signals within tumors via the use of an OX40 agonist antibody.

To test this hypothesis, GFP mice bearing well-established MCA205 tumors were treated with anti-OX40 mAb or control rat IgG antibody. Seven days later we analyzed the TIL and dLNs. We observed a small but significant increase in GFPhi CD8 T cells in the dLN ($p=0.0102$) but an even greater increase in GFPhi T cells in the tumor ($p<0.0001$) (Figure 5D) again suggesting that at the time of harvest the majority of tumor antigen specific T cells are encountering their ligand *in situ* rather than in the tumor dLN.

OX40 agonists are in clinical trials for the treatment of patients with late stage cancer. Therefore, we next asked how an OX40 agonist antibody compared with checkpoint blockade in regards to the expansion of CD8 GFPhi TIL. In particular, we compared anti-CTLA4, anti-PD-1, anti-PDL1 and anti-OX40 mAbs. We hypothesized that because the anti-OX40 mAb is an agonist, previously shown to promote the proliferation and survival of antigen specific T cells, it would be superior in regards to its ability to expand tumor resident CD8 T cells receiving strong TCR signals as compared to the other 3 mAbs.

Therefore, we inoculated GFP animals with MCA205 tumors on each flank and once tumors were established (~10–12 days later), treated the animals with a total of 500 μg anti-OX40 or anti-CTLA4, or control rat IgG (in two injections) or 600 μg anti-PD-1 or anti-PDL1 mAbs (in three injections) over seven days. Interestingly, at day seven after the start of treatment, anti-OX40 and anti-CTLA4 treatment led to a two-fold increase in the frequency of CD8 T cells receiving strong TCR signals (GFPhi) and this was observed in the tumor but not the spleen (Figure 5E). However, anti-PD-1 and anti-PD-L1 had minimal effect on increasing the percentage of GFPhi T cells in the tumor (Figure 5E) even though CD8+GFPhi TIL co-express PD-1 (Figure 3A) and this tumor expresses PD-L1.

OX40 mediated expansion of Nur77GFPhi CD8 T cells is transient

Previous work from our group has shown that early treatment of tumor bearing mice with an OX40 agonist promotes their long-term survival (25). In an effort to better understand the mechanism by which OX40 agonists enhance anti-tumor responses in this vaccination-like setting, we treated MCA205 tumor bearing mice shortly after tumor implantation (day 5, 9). At the time of harvest (day 10), there was an almost 4-fold increase in total and GFPhi CD8 T cells in the dLN of tumor bearing animals (Figure 6A). At this same time point, however, there was only a subtle increase in the frequency of GFPhi CD8 T cells within the tumor (Figure 6B). However, their total MFI was significantly higher than the untreated control population of CD8 T cells. Importantly, this early treatment and enhanced expansion of CD8 T cells with high affinity TCRs for tumor-associated antigens protected ~60% of these animals from death (Figure 6C).

Given that OX40 agonists are in clinical trials to treat patients with advanced tumors rather than in a prophylactic-like setting (such as described above), we next asked about the ability of an OX40 agonist to expand pre-existing CD8 T cell responses. To this point, we have previously shown that in patients being treated with an OX40 agonist, there is an increase in the proliferation (as measured by Ki67+) of peripheral CD8+ T cells (28). However, whether this proliferation was antigen-dependent or independent was unclear. Therefore, we next addressed whether proliferation of CD8+ T cells in well-established tumors was in the GFPhi vs GFPlo population following treatment with anti-OX40 antibody (Figure 6D). Consistent with our observations in patients treated with an OX40 agonist antibody, we observed a significant increase in Ki67+ CD8 T cells in the tumor (Figure 6E). In fact, there was a 5-fold increase in the Ki67+GFPhi population of CD8 T cells in the tumor following anti-OX40 treatment (Figure 6F) suggesting that in the tumor microenvironment we can detect proliferating high affinity T cells whose TCRs were recently ligated. Importantly, this 5-fold increase in CD8 TIL with high affinity TCRs also prolonged the survival of MCA205 tumor bearing mice as compared to the control treated animals (Figure 6G). Interstingly, the majority of proliferating T cells in the tumors of treated or untreated animals were GFPlow (Figure 6E). While this observation was initially surprising to us, it is reminiscent of work in viral infection models which established that proliferation of naïve and effector CD8 T cells can happen in a bystander fashion, independent of antigen encounter (45, 46). Moreover, using a similar Nur77GFP model, proliferating T cells were shown to retain their Nur77GFPhi status after αντι−CD3 ligation as long as the antibody was present (38). Given our observation that anywhere from 10–75% of endogenous tumor antigen specific T cells are GFPhi at any point in time (Figure 3B), it is also possible that the Ki67+GFPlow T cells were driven to proliferate after strong TCR encounters but the limited availability of antigen has led to a decay in GFP.

After observing an increase in the CD8+Ki67+GFPhi population of TIL, we investigated the kinetics of the expansion of GFPhi T cells after anti-OX40 immunotherapy. A modified experimental design to that described in Figure 6D was used to assess the proliferative potency of a single injection (as compared to 2 injections) of anti-OX40 in mice bearing MCA205 tumors (~10 days post tumor inoculation). Tumor infiltrating CD8 T cells (Figure 6H) and dLNs (Figure 6I) were harvested at serial time points post treatment for analysis.

Four days after immunotherapy treatment we detected an increase in GFPhi CD8+ TIL and these cells increased over the next 4–5 days peaking approximately nine days after antibody administration (Figure 6H). The population of GFPhi T cells was stable between day 7 and day 9 and contracted by day 13.

The kinetics of the expansion of GFPhi T cells in the tumor raised the possibility that newly primed tumor-antigen specific T cells were trafficking from the dLN into the tumor after antigen encounter. Previous studies have suggested that naïve T cells dwell in the dLN for anywhere from 12–18 hrs after antigen encounter before egressing (47). Therefore, we predicted that if tumor-antigen specific CD8 T cell activation occurred in the dLN, there should be an increase in GFPhi T cells in the dLN with similar kinetics to that observed in the tumor. However, when we calculated the frequency of GFPhi T cells in the tumor dLNs at these same time points, we found no significant increase in the frequency of GFPhi T cells (Figure 6I) over the duration of the study. Together, this suggests that in well-established tumors, the OX40+CD8+ T cells that are reactive for tumor antigens reside within the tumor and are expanded *in situ*.

OX40 immunotherapy maintains the anti-tumor function of adoptively transferred CD8 T cells

Previous work has established that anti-OX40 mAb immunotherapy can restore the function of self and tumor antigen tolerized CD8 T cells (27, 48). Given this result, we hypothesized that the increase in CD8+GFPhi T cells in the tumor could be the result of 1) proliferation of pre-existing OX40+ T cells and/or 2) sustained TCR signaling and Nur77GFP induction in tolerized T cells with high affinity TCRs. To address these questions, we adoptively transferred OT-I/Thy1.1/Nur77GFP T cells into well established MCA205-WT or MCA205-OVA tumor bearing mice. Animals were treated with anti-OX40 mAb or rat IgG on days 1 and 5 after OT-I transfer and tumors were harvested a day or a week after the last antibody administration (Figure 7A). Consistent with the fidelity of the tumor antigen specific GFP upregulation reported in Figure 2, at day 6 after OT-I adoptive transfer, only those CD8 T cells recovered from OVA-bearing tumors were GFPhi (Figure 7B top right). Of note, anti-OX40 mAb treatment did not increase the total GFP MFI of the OT-I T cells in OVA-bearing tumors suggesting that the Nur77 BAC transgene is not directly regulated by OX40 ligation. In contrast to the GFPhi expression on OT-I T cells in OVA bearing tumors at day 6 post adoptive transfer (AT), by day thirteen after AT, the GFP signal on the tumor isolated OT-I's was greatly decreased, identical levels to that of OT-I's isolated from WT tumors (Figure 7B, bottom left). OX40 agonist but not the control antibody partially maintained the induction of GFP on OT-I T cells in OVA-bearing tumors at day 13 after antibody administration (Figure 7B, bottom right). Interestingly, not all OT-I T cells were GFPhi after anti-OX40 therapy.

In addition, while we observed many large tumors (~100mm^2) initially regress with adoptive T cell therapy alone (Figure 7C), this therapy alone had limited efficacy (~9% or 1/11 cured tumors) (Figure 7D). However, in those animals treated with adoptive T cell therapy and anti-OX40 mAb immunotherapy, we observed a significant increase in large tumor regression and disease free survival (~70% of animals cured tumors >50mm^2 8/11) (Figure 7C bottom, 7D). Taken together, it is plausible that anti-OX40 mAb immunotherapy 1)

maintains the function of or 2) prevents the tolerization of tumor-antigen specific CD8 T cells (27, 48), some of which express high affinity TCRs.

Discussion

Studies of tumor antigen specific T cell responses have largely relied on adoptive transfers of TCR transgenic T cells and the forced expression of foreign antigens by tumor cells. Furthermore, until recently, there were very few tools available for interrogating the TCR signal strength of the polyclonal anti-tumor immune response. Yet generating high affinity anti-tumor CD8 T cell responses is the goal of many immunotherapies to date. Therefore, laboratories have historically relied upon the activation markers CD69 and CD44 to identify antigen experienced polyclonal T cells within the tumor (49). More recently, others have used PD-1 expression to identify tumor-reactive T cells (14). In this study, we introduce a novel tool to assess the productive engagement of polyclonal T cell receptors and the natural affinities of some of these receptors for endogenous tumor-associated antigens. We present evidence that traditional markers of T cell activation (CD69, CD44, PD-1) are unreliable markers of recent antigen exposure within the tumor because they can be induced in the tumor microenvironment in the absence of the T cells' cognate ligand.

While CD69 and CD44 up-regulation within the tumor was somewhat predictable due to previous work indicating the TCR-independent bystander induction of these molecules on antigen-inexperienced T cells (33), cytokines and hormones have only been described to influence TCR-independent PD-1 expression on non-lymphocyte hematopoietic derived cells (50, 51). Cognate antigen receptor ligation is described as being required for the initial up-regulation of PD-1 on naïve lymphocytes and its expression can be further enhanced by cytokines such as TGFβ or type I interferons (52–55). In fact, in eloquent work using a chronic viral infection model, Ahmed's group highlighted the continued epitope recognition requirement for PD-1 maintenance on antigen specific CD8 T cells (56). Given this previously established requirement for TCR:pMHC interaction for PD-1 upregulation and it's induction soon after TCR ligation (57), we initially assessed PD-1 expression on CD8+GFPhi T cells within the tumor in an effort to identify a faithful combination of cell surface molecules that distinguish antigen specific T cells from bystander activated T cells. However, we found nearly equivalent expression of PD-1 on antigen inexperienced OT-I T cells in mice bearing MCA205 wild-type versus antigen experienced OT-Is residing in OVA-expressing tumors. While there was a significant increase in the total number of OT-I T cells that infiltrated the OVA bearing tumor, the Nur77GFP reporter was the only marker in these studies that faithfully identified TCR activation through antigen engagement. Moreover, the isolation of OT-I T cells from non-OVA expressing tumors is reminiscent of previously published work that highlighted that the inflammatory tumor microenvironment can recruit naïve 'bystander' CD8 T cells in the absence of cognate antigen (41). This observation is also supported in models of chronic viral infection, where naïve 'bystander' T cells are reported to enter the inflamed tissue and appear antigen specific (via expression of CD44 or CD69) (58, 59) and others have reported the masquerading of naïve CD8 T cells as memory T cells through proliferation and CD44 upregulation (46). Taken together, these findings reinforce the need to identify faithful markers of TCR ligation that are not induced by inflammation within the tumor. Moreover, given our observation that the tumor associated

cytokine milieu can upregulate PD-1, we challenge the interpretation that all PD-1 positive T cells in the tumor can be regarded as tumor antigen specific. This finding has profound implications for the current anti-PD-1 immunotherapy rationale in various cancer patient populations.

Given that anti-tumor immune responses can be regulated by the availability of co-stimulation, we then used this tool to unveil novel mechanisms of action of agonist OX40 mAb immunotherapy. We demonstrate that CD8+Nur77GFPhi T cells are enriched for OX40 expression and OX40 ligation with an agonist antibody plays a pivotal role in maintaining the overall magnitude and longevity of the high affinity anti-tumor immune response (Figure 6). When animals were treated shortly after tumor inoculation (within the first 3–5 days), there was a 4-fold increase in the number of total and high affinity CD8 T cells in the dLNs but not in the tumor of anti-OX40 mAb treated animals. We were initially surprised at the rather insignificant increase in the frequency of GFPhi T cells in the tumor. However, given that this early treatment regimen somewhat mimics a prophylactic or vaccination like setting, it was not surprising that an OX40 agonist could boost the priming of antigen-specific T cells of which only a few had trafficked back into the tumor. This enhanced priming of high affinity CD8 T cells also supported the long term survival of ~60% of the anti-OX40 mAb treated animals (Figure 6C). Interestingly, when tumor-bearing animals were treated much later (day 10–12), when anti-OX40 mAb immunotherapy could not cure the tumors but only extend the animals life (Figure 6G), the expansion of CD8 T cells with high affinity TCRs was restricted to the tumor (Figure 6H) and was transient. Taken together, this suggests that OX40 agonists, when provided in the context of well-established progressing tumors such as that seen in the clinic, may enhance the *in situ* function and proliferation of tumor-antigen specific CD8 T cells. This data is consistent with a role for OX40 co-stimulatory signals in promoting the survival of antigen specific T cells in a Bcl-xl/Bcl-2 dependent fashion (60).

Using the OT-I/Kb:OVA model system we demonstrate the ability of agonist OX40 mAb immunotherapy to maintain the NFAT-mediated upregulation of the immediate early gene Nur77 on non-functional (as demonstrated by inability to produce IFNγ upon anti-CD3 mAb stimulation), tumor infiltrating, CD8 T cells. Interestingly, the Weiss group recently published a study in which they demonstrated the sustained expression of Nur77GFP in proliferating T cells after *in vitro* anti-CD3 mAb stimulation however, after TCR stimulation *in vivo*, there was a progressive decline of GFP expression in proliferating daughter cells. Together, this suggests that when pMHC or dwell time with antigen presenting cells (APCs) is abundant, then the GFPhi Ki67+ CD8 T cells reflect the strength of activating signals that initiated their proliferation. However, if pMHC is limited or tumor infiltrating CD8 T cells move away from an APC, then GFP expression will decay with proliferation. Importantly, this work highlights that sustained pMHC:TCR interaction is not necessary for proliferation of T cells. This is an important observation given the ability of OX40 agonists to enhance the proliferation of both GFPhi and GFPlow CD8 T cells in the tumor (Figure 6E). It is plausible that the enhanced GFP expression in a subpopulation of proliferating CD8 T cells in the tumor after agonist OX40 immunotherapy reflects maintained NFAT-mediated GFP expression as observed in the OT-I adoptive cell therapy experiments (Figure 7). Another interesting observation from the Weiss groups' findings is that they could modulate the level

of Nur77GFP induction after anti-CD3 mAb stimulation of T cells by treating the cells with a small molecule kinase inhibitor of Zap70 (38). They could significantly abrogate GFP induction by a strong TCR stimulus by inhibiting Zap70 kinase activity. This observation together with our data that OT-I T cells have sustained GFP expression after adoptive transfer and anti-OX40 immunotherapy into tumor bearing animals (Figure 7B), suggests a possible role for OX40 agonist immunotherapy in maintaining proximal TCR signaling in chronically stimulated, tumor-infiltrating T cells.

The rapid on/off kinetics of Nur77GFP expression provided us with a unique ability to assess *in situ* TCR ligation and the affinity of these interactions. However, we recognize there are limitations to the Nur77GFP system as a tool for assessing tumor antigen specific T cell responses. First, due to the decay of GFP after pMHC:TCR disassociation and the loss of GFP up-regulation on chronically stimulated antigen specific T cells, we believe our data underestimates the frequency of high affinity T cell clones that exist in the tumor microenvironment. In fact, we observed differences in the induction of Nur77GFP on endogenous tumor-antigen specific T cells as compared to adoptively transferred T cells. Only ~75% of the OVA tetramer positive cells were GFPhi 7 days after tumor inoculation where as 5 days after OT-I/Nur77GFP adoptive transfer, 95% of cells were GFPhi (Figure 2, Figure 3). This difference could reflect the asynchronous nature of the endogenous CD8 T cell response to tumor antigens as compared to the synchronized adoptive transfer of OT-I T cells or the decay of GFP that happens over 48 hours. Second, we accept that there are lower affinity tumor antigen specific responses that we are unable to detect given the lack of synchronization of T cell exposure to antigen in our *in vivo* assays. In fact, previous work with the Nur77GFP model suggests that this experimental tool is most sensitive for distinguishing differences in low affinity T cell responses (22). However, differentiating these low affinity T cell responses to tumor-associated antigens from decaying high affinity signals proves challenging.

In addition to revealing the affinity of endogenous tumor-associated antigens, it is also plausible that the Nur77GFP model could be used to monitor candidate tumor-associated antigens in tumor antigen screens. Such assays would provide qualitative indicators of the TCR signal strength for potential neo-antigens and when coupled with CD69 expression and/or proliferation, might reveal the potency of such neo-antigens to cross the signaling threshold necessary for optimal T cell activation.

To our surprise, anti-OX40 and anti-CTLA4 mAb therapies were unique in their ability to increase the percentage of GFPhi T cells when compared to anti-PD-1 or anti-PD-L1. While we propose that the elevated expression of OX40 on CD8+GFPhi T cells contributes to the expanded population of CD8+ high affinity T cells within the tumor, recent work from Sarkars' group could provide a possible explanation for the anti-CTLA4 observation. They highlight the ability of CTLA4, expressed by regulatory T cells, to restrain memory CD8 T cells in a quiescent state (61). Given that anti-CTLA4 therapy has been shown to deplete tumor associated regulatory T cells in mice (62), the increase in CD8+GFPhi T cells with this therapy might reflect a re-invigoration of memory CD8 T cells, some of which have high affinity TCRs. These observations also suggest that anti-OX40 plus anti-CTLA4 mAbs as a combination immunotherapy might further increase the frequency of tumor antigen

specific T cells within the tumor. These questions are under further investigation within our laboratory.

Finally, of interest to the studies herein was whether chronically stimulated tumor antigen specific CD8 T cells would continue to report the affinity of their tumor-associated tolerizing antigen. The Nur77GFP transgenic system has been used in studies of T cell function and tolerance. Self-reactive, anergic CD4+CD44+Foxp3- T cells are reported to remain GFPhi despite their lack of effector function (63). However, in these studies, antigen specific CD8 T cells were not studied. Therefore, we were surprised to observe that OT-I TCR transgenic T cells undergoing chronic stimulation by a tumor antigen lose their ability to up-regulate the GFP transgene despite the presence of antigen and normal TCR expression. This observation, however, provided an intriguing method to interrogate the mechanism of action of OX40 in regards to TCR signaling, prolonging effective adoptive cell therapy, and anti-tumor immunity. Our initial observation after adoptive transfer of OT-I T cells was a decrease in tumor size. Some animals had complete responses and tumors were no longer detectable (~10% of control treated) while others achieved delayed tumor growth (Figure 7C and D) but ultimately had to be euthanized due to tumor burden. Surprisingly, those animals that received adoptive cell therapy and were concurrently treated with agonist anti-OX40 mAb immunotherapy, had a significant increase in tumor regression of large tumors and overall long term survival (~70% long term survival). Given our prior observation that chronically stimulated OT-I T cells were no longer able to upregulate GFP, suggesting an interruption in TCR-induced NFAT signaling, we were surprised to observe such profound anti-tumor responses in the animals treated with adoptive cell therapy combined with anti-OX40 mAb (Figure 7C). However, upon analysis of OT-I T cells within the tumor at approximately day 13 after AT, there was a partial stabilization of GFP up-regulation in anti-OX40 treated animals but not in the control treated animals. This observation and the mixed tumor response in the MCA205-OVA bearing mice, when taken together, are consistent with a model where the integration of TCR signals is a stochastic response of each individual T cell and not a population decision. This finding is consistent with recent data from the Weiss group using their own Nur77GFP reporter mouse that proposed that the integration of a high affinity TCR signal amongst a monoclonal population of T cells is unique to each TCR clone with some clones reaching the Nur77GFPhi and TCR signaling threshold before others (38). This stochastic integration of TCR signals by tumor-antigen specific T cells might also help explain the differences in GFP expression in tetramer positive T cells in the tumor (Figure 3B). Together, this data suggests that adoptive cell therapy combined with OX40 agonist immunotherapy might be a profound combination by which to prolong signaling pathways downstream of productive TCR interactions or even rescue adoptive cell therapy in the clinic. We are currently investigating whether other immunotherapies as single agents or in combination will also maintain the TCR-mediated NFAT regulation of GFP expression on tumor infiltrating CD8 T cells in an effort to guide the rational combination of immunotherapy agents for clinical use.

Acknowledgments

We thank Drs. Walter Urba and Michael Gough for critical review of the manuscript, Drs. Ann Hill, David Parker, and Susan Murray for their thoughtful discussions, and the EACRI-CRAD vivarium staff for animal husbandry. We

also thank the NIH Tetramer Facility for generating H-2Db and H-2Kb tetramers for use within studies presented in this manuscript.

Grant support: AE Moran was supported by NIH T32 AI078903 and by the American Cancer Society PF-14-053-01. A.D. Weinberg was supported in part by NIH Grant 5R01CA102577, a commercial research grant from MedImmune, and the Providence Medical Foundation.

Abbreviations used in this article

PD-1	programmed death 1
PD-L1	programmed death-ligand 1
WT	wild-type
Tg	transgenic
B16	B16F10
MCA	3’-methylcholanthrene
MCA	3-methylcholanthrene induced
pMHC	peptide MHC
AT	Adoptive transfer
GFP	Nur77GFP

References

1. Zehn D, Lee SY, Bevan MJ. Complete but curtailed T-cell response to very low-affinity antigen. Nature. 2009; 458:211–214. [PubMed: 19182777]
2. Schumacher TN, Schreiber RD. Neoantigens in cancer immunotherapy. Science. 2015; 348:69–74. [PubMed: 25838375]
3. Gubin MM, Zhang X, Schuster H, Caron E, Ward JP, Noguchi T, Ivanova Y, Hundal J, Arthur CD, Krebber WJ, Mulder GE, Toebes M, Vesely MD, Lam SS, Korman AJ, Allison JP, Freeman GJ, Sharpe AH, Pearce EL, Schumacher TN, Aebersold R, Rammensee HG, Melief CJ, Mardis ER, Gillanders WE, Artyomov MN, Schreiber RD. Checkpoint blockade cancer immunotherapy targets tumour-specific mutant antigens. Nature. 2014; 515:577–581. [PubMed: 25428507]
4. Kreiter S, Vormehr M, van de Roemer N, Diken M, Lower M, Diekmann J, Boegel S, Schrors B, Vascotto F, Castle JC, Tadmor AD, Schoenberger SP, Huber C, Tureci O, Sahin U. Mutant MHC class II epitopes drive therapeutic immune responses to cancer. Nature. 2015; 520:692–696. [PubMed: 25901682]
5. Coulie PG, Lehmann F, Lethe B, Herman J, Lurquin C, Andrawiss M, Boon T. A mutated intron sequence codes for an antigenic peptide recognized by cytolytic T lymphocytes on a human melanoma. Proceedings of the National Academy of Sciences of the United States of America. 1995; 92:7976–7980. [PubMed: 7644523]
6. Wolfel T, Hauer M, Schneider J, Serrano M, Wolfel C, Klehmann-Hieb E, De Plaen E, Hankeln T, Meyer zum Buschenfelde KH, Beach D. A p16INK4a–insensitive CDK4 mutant targeted by cytolytic T lymphocytes in a human melanoma. Science. 1995; 269:1281–1284. [PubMed: 7652577]
7. Rizvi NA, Hellmann MD, Snyder A, Kvistborg P, Makarov V, Havel JJ, Lee W, Yuan J, Wong P, Ho TS, Miller ML, Rekhtman N, Moreira AL, Ibrahim F, Bruggeman C, Gasmi B, Zappasodi R, Maeda Y, Sander C, Garon EB, Merghoub T, Wolchok JD, Schumacher TN, Chan TA. Cancer immunology.

Mutational landscape determines sensitivity to PD-1 blockade in non-small cell lung cancer. Science. 2015; 348:124–128. [PubMed: 25765070]

8. Robbins PF, Lu YC, El-Gamil M, Li YF, Gross C, Gartner J, Lin JC, Teer JK, Cliften P, Tycksen E, Samuels Y, Rosenberg SA. Mining exomic sequencing data to identify mutated antigens recognized by adoptively transferred tumor-reactive T cells. Nature medicine. 2013; 19:747–752.
9. van Rooij N, van Buuren MM, Philips D, Velds A, Toebes M, Heemskerk B, van Dijk LJ, Behjati S, Hilkmann H, El Atmioui D, Nieuwland M, Stratton MR, Kerkhoven RM, Kesmir C, Haanen JB, Kvistborg P, Schumacher TN. Tumor exome analysis reveals neoantigen-specific T-cell reactivity in an ipilimumab-responsive melanoma. Journal of clinical oncology : official journal of the American Society of Clinical Oncology. 2013; 31:e439–e442. [PubMed: 24043743]
10. Tran E, Ahmadzadeh M, Lu YC, Gros A, Turcotte S, Robbins PF, Gartner JJ, Zheng Z, Li YF, Ray S, Wunderlich JR, Somerville RP, Rosenberg SA. Immunogenicity of somatic mutations in human gastrointestinal cancers. Science. 2015; 350:1387–1390. [PubMed: 26516200]
11. Tran E, Turcotte S, Gros A, Robbins PF, Lu YC, Dudley ME, Wunderlich JR, Somerville RP, Hogan K, Hinrichs CS, Parkhurst MR, Yang JC, Rosenberg SA. Cancer immunotherapy based on mutation-specific CD4+ T cells in a patient with epithelial cancer. Science. 2014; 344:641–645. [PubMed: 24812403]
12. Zhai Y, Yang JC, Spiess P, Nishimura MI, Overwijk WW, Roberts B, Restifo NP, Rosenberg SA. Cloning and characterization of the genes encoding the murine homologues of the human melanoma antigens MART1 and gp100. Journal of immunotherapy. 1997; 20:15–25. [PubMed: 9101410]
13. Alexander RB, Fitzgerald EB, Mixon A, Carter CS, Jakobsen M, Cohen PA, Rosenberg SA. Helper T cells infiltrating human renal cell carcinomas have the phenotype of activated memory-like T lymphocytes. Journal of immunotherapy with emphasis on tumor immunology : official journal of the Society for Biological Therapy. 1995; 17:39–46.
14. Gros A, Robbins PF, Yao X, Li YF, Turcotte S, Tran E, Wunderlich JR, Mixon A, Farid S, Dudley ME, Hanada K, Almeida JR, Darko S, Douek DC, Yang JC, Rosenberg SA. PD-1 identifies the patient-specific CD8(+) tumor-reactive repertoire infiltrating human tumors. The Journal of clinical investigation. 2014; 124:2246–2259. [PubMed: 24667641]
15. Overwijk WW, Tsung A, Irvine KR, Parkhurst MR, Goletz TJ, Tsung K, Carroll MW, Liu C, Moss B, Rosenberg SA, Restifo NP. gp100/pmel 17 is a murine tumor rejection antigen: induction of "self"-reactive, tumoricidal T cells using high-affinity, altered peptide ligand. J Exp Med. 1998; 188:277–286. [PubMed: 9670040]
16. Shiow LR, Rosen DB, Brdickova N, Xu Y, An J, Lanier LL, Cyster JG, Matloubian M. CD69 acts downstream of interferon-alpha/beta to inhibit S1P1 and lymphocyte egress from lymphoid organs. Nature. 2006; 440:540–544. [PubMed: 16525420]
17. Sun S, Zhang X, Tough DF, Sprent J. Type I interferon-mediated stimulation of T cells by CpG DNA. J Exp Med. 1998; 188:2335–2342. [PubMed: 9858519]
18. Godfrey WR, Fagnoni FF, Harara MA, Buck D, Engleman EG. Identification of a human OX-40 ligand, a costimulator of CD4+ T cells with homology to tumor necrosis factor. J Exp Med. 1994; 180:757–762. [PubMed: 7913952]
19. Baldwin TA, Hogquist KA. Transcriptional analysis of clonal deletion in vivo. Journal of immunology. 2007; 179:837–844.
20. Winoto A, Littman DR. Nuclear hormone receptors in T lymphocytes. Cell. 2002; (109 Suppl):S57–S66. [PubMed: 11983153]
21. Zikherman J, Parameswaran R, Weiss A. Endogenous antigen tunes the responsiveness of naive B cells but not T cells. Nature. 2012; 489:160–164. [PubMed: 22902503]
22. Moran AE, Holzapfel KL, Xing Y, Cunningham NR, Maltzman JS, Punt J, Hogquist KA. T cell receptor signal strength in Treg and iNKT cell development demonstrated by a novel fluorescent reporter mouse. J Exp Med. 2011; 208:1279–1289. [PubMed: 21606508]
23. Paterson DJ, Jefferies WA, Green JR, Brandon MR, Corthesy P, Puklavec M, Williams AF. Antigens of activated rat T lymphocytes including a molecule of 50,000 Mr detected only on CD4 positive T blasts. Molecular immunology. 1987; 24:1281–1290. [PubMed: 2828930]

24. Montler R, Bell RB, Thalhofer C, Leidner R, Feng Z, Fox BA, Cheng AC, Bui TG, Tucker C, Hoen H, Weinberg A. OX40, PD-1 and CTLA-4 are selectively expressed on tumor-infiltrating T cells in head and neck cancer. Clinical & translational immunology. 2016; 5:e70. [PubMed: 27195113]
25. Weinberg AD, Rivera MM, Prell R, Morris A, Ramstad T, Vetto JT, Urba WJ, Alvord G, Bunce C, Shields J. Engagement of the OX-40 receptor in vivo enhances antitumor immunity. Journal of immunology. 2000; 164:2160–2169.
26. Ruby CE, Redmond WL, Haley D, Weinberg AD. Anti-OX40 stimulation in vivo enhances CD8+ memory T cell survival and significantly increases recall responses. European journal of immunology. 2007; 37:157–166. [PubMed: 17183611]
27. Redmond WL, Gough MJ, Weinberg AD. Ligation of the OX40 co-stimulatory receptor reverses self-Ag and tumor-induced CD8 T-cell anergy in vivo. European journal of immunology. 2009; 39:2184–2194. [PubMed: 19672905]
28. Brendan D, Curti MK-B, Morris Nicholas, Walker Edwin, Chisholm Lana, Flloyd Kevin, Walker Joshua, Gonzales Iliana, Meeuwsen Tanisha, Fox Bernard A, Modgil Tarsem, Miller William, Haley Daniel, Coffey Todd, Fisher Brenda, Delanty-Miller Laurie, Rymarchyk Nicole, Kelly Tracy, Crocenzi Todd, Bernstein Eric, Sanborn Rachel, Urba Walter J, Weinberg Andrew D. OX40 is a potent immune stimulating target in late stage cancer patients. Cancer research. 2013; 73:7189–7198. [PubMed: 24177180]
29. Lees JR, Charbonneau B, Swanson AK, Jensen R, Zhang J, Matusik R, Ratliff TL. Deletion is neither sufficient nor necessary for the induction of peripheral tolerance in mature CD8+ T cells. Immunology. 2006; 117:248–261. [PubMed: 16423061]
30. Mackay LK, Braun A, Macleod BL, Collins N, Tebartz C, Bedoui S, Carbone FR, Gebhardt T. Cutting edge: CD69 interference with sphingosine-1-phosphate receptor function regulates peripheral T cell retention. Journal of immunology. 2015; 194:2059–2063.
31. Liu F, Whitton JL. Cutting edge: re-evaluating the in vivo cytokine responses of CD8+ T cells during primary and secondary viral infections. Journal of immunology. 2005; 174:5936–5940.
32. Balkwill F, Mantovani A. Inflammation and cancer: back to Virchow? Lancet. 2001; 357:539–545. [PubMed: 11229684]
33. Coussens LM, Werb Z. Inflammation and cancer. Nature. 2002; 420:860–867. [PubMed: 12490959]
34. Lanier LL, Buck DW, Rhodes L, Ding A, Evans E, Barney C, Phillips JH. Interleukin 2 activation of natural killer cells rapidly induces the expression and phosphorylation of the Leu-23 activation antigen. J Exp Med. 1988; 167:1572–1585. [PubMed: 3259252]
35. Oppenheimer-Marks N, Davis LS, Lipsky PE. Human T lymphocyte adhesion to endothelial cells and transendothelial migration. Alteration of receptor use relates to the activation status of both the T cell and the endothelial cell. Journal of immunology. 1990; 145:140–148.
36. Hogquist KA, Jameson SC, Heath WR, Howard JL, Bevan MJ, Carbone FR. T cell receptor antagonist peptides induce positive selection. Cell. 1994; 76:17–27. [PubMed: 8287475]
37. Fasso M, Waitz R, Hou Y, Rim T, Greenberg NM, Shastri N, Fong L, Allison JP. SPAS-1 (stimulator of prostatic adenocarcinoma-specific T cells)/SH3GLB2: A prostate tumor antigen identified by CTLA-4 blockade. Proceedings of the National Academy of Sciences of the United States of America. 2008; 105:3509–3514. [PubMed: 18303116]
38. Au-Yeung BB, Zikherman J, Mueller JL, Ashouri JF, Matloubian M, Cheng DA, Chen Y, Shokat KM, Weiss A. A sharp T-cell antigen receptor signaling threshold for T-cell proliferation. Proceedings of the National Academy of Sciences of the United States of America. 2014; 111:E3679–E3688. [PubMed: 25136127]
39. Ahmed R, Gray D. Immunological memory and protective immunity: understanding their relation. Science. 1996; 272:54–60. [PubMed: 8600537]
40. Slifka MK, Rodriguez F, Whitton JL. Rapid on/off cycling of cytokine production by virus-specific CD8+ T cells. Nature. 1999; 401:76–79. [PubMed: 10485708]
41. Thompson ED, Enriquez HL, Fu YX, Engelhard VH. Tumor masses support naive T cell infiltration, activation, and differentiation into effectors. J Exp Med. 2010; 207:1791–1804. [PubMed: 20660615]

42. Bansal-Pakala P, Halteman BS, Cheng MH, Croft M. Costimulation of CD8 T cell responses by OX40. Journal of immunology. 2004; 172:4821–4825.
43. Kotani A, Ishikawa T, Matsumura Y, Ichinohe T, Ohno H, Hori T, Uchiyama T. Correlation of peripheral blood OX40+(CD134+) T cells with chronic graft-versus-host disease in patients who underwent allogeneic hematopoietic stem cell transplantation. Blood. 2001; 98:3162–3164. [PubMed: 11698307]
44. Klinger M, Kim JK, Chmura SA, Barczak A, Erle DJ, Killeen N. Thymic OX40 expression discriminates cells undergoing strong responses to selection ligands. Journal of immunology. 2009; 182:4581–4589.
45. Kaech SM, Ahmed R. Memory CD8+ T cell differentiation: initial antigen encounter triggers a developmental program in naive cells. Nature immunology. 2001; 2:415–422. [PubMed: 11323695]
46. Murali-Krishna K, Ahmed R. Cutting edge: naive T cells masquerading as memory cells. Journal of immunology. 2000; 165:1733–1737.
47. Mempel TR, Henrickson SE, Von Andrian UH. T-cell priming by dendritic cells in lymph nodes occurs in three distinct phases. Nature. 2004; 427:154–159. [PubMed: 14712275]
48. Song A, Tang X, Harms KM, Croft M. OX40 and Bcl-xL promote the persistence of CD8 T cells to recall tumor-associated antigen. Journal of immunology. 2005; 175:3534–3541.
49. Berd D, Maguire HC Jr, Mastrangelo MJ, Murphy G. Activation markers on T cells infiltrating melanoma metastases after therapy with dinitrophenyl-conjugated vaccine. Cancer immunology, immunotherapy : CII. 1994; 39:141–147. [PubMed: 7923243]
50. Kinter AL, Godbout EJ, McNally JP, Sereti I, Roby GA, O'Shea MA, Fauci AS. The common gamma-chain cytokines IL-2, IL-7, IL-15, and IL-21 induce the expression of programmed death-1 and its ligands. Journal of immunology. 2008; 181:6738–6746.
51. Polanczyk MJ, Hopke C, Vandenbark AA, Offner H. Estrogen-mediated immunomodulation involves reduced activation of effector T cells, potentiation of Treg cells, and enhanced expression of the PD-1 costimulatory pathway. Journal of neuroscience research. 2006; 84:370–378. [PubMed: 16676326]
52. Terawaki S, Chikuma S, Shibayama S, Hayashi T, Yoshida T, Okazaki T, Honjo T. IFN-alpha directly promotes programmed cell death-1 transcription and limits the duration of T cell-mediated immunity. Journal of immunology. 2011; 186:2772–2779.
53. Gerner MY, Heltemes-Harris LM, Fife BT, Mescher MF. Cutting edge: IL-12 and type I IFN differentially program CD8 T cells for programmed death 1 re-expression levels and tumor control. Journal of immunology. 2013; 191:1011–1015.
54. Rekik R, Belhadj Hmida N, Ben Hmid A, Zamali I, Kammoun N, Ben Ahmed M. PD-1 induction through TCR activation is partially regulated by endogenous TGF-beta. Cellular & molecular immunology. 2015; 12:648–649. [PubMed: 25363526]
55. Vanpouille-Box C, Diamond JM, Pilones KA, Zavadil J, Babb JS, Formenti SC, Barcellos-Hoff MH, Demaria S. TGFbeta Is a Master Regulator of Radiation Therapy-Induced Antitumor Immunity. Cancer research. 2015; 75:2232–2242. [PubMed: 25858148]
56. Blattman JN, Wherry EJ, Ha SJ, van der Most RG, Ahmed R. Impact of epitope escape on PD-1 expression and CD8 T-cell exhaustion during chronic infection. Journal of virology. 2009; 83:4386–4394. [PubMed: 19211743]
57. Agata Y, Kawasaki A, Nishimura H, Ishida Y, Tsubata T, Yagita H, Honjo T. Expression of the PD-1 antigen on the surface of stimulated mouse T and B lymphocytes. International immunology. 1996; 8:765–772. [PubMed: 8671665]
58. Tough DF, Borrow P, Sprent J. Induction of bystander T cell proliferation by viruses and type I interferon in vivo. Science. 1996; 272:1947–1950. [PubMed: 8658169]
59. Unutmaz D, Pileri P, Abrignani S. Antigen-independent activation of naive and memory resting T cells by a cytokine combination. J Exp Med. 1994; 180:1159–1164. [PubMed: 8064232]
60. Rogers PR, Song J, Gramaglia I, Killeen N, Croft M. OX40 promotes Bcl-xL and Bcl-2 expression and is essential for long-term survival of CD4 T cells. Immunity. 2001; 15:445–455. [PubMed: 11567634]

61. Kalia V, Penny LA, Yuzefpolskiy Y, Baumann FM, Sarkar S. Quiescence of Memory CD8(+) T Cells Is Mediated by Regulatory T Cells through Inhibitory Receptor CTLA-4. Immunity. 2015; 42:1116–1129. [PubMed: 26084026]

62. Simpson TR, Li F, Montalvo-Ortiz W, Sepulveda MA, Bergerhoff K, Arce F, Roddie C, Henry JY, Yagita H, Wolchok JD, Peggs KS, Ravetch JV, Allison JP, Quezada SA. Fc-dependent depletion of tumor-infiltrating regulatory T cells co-defines the efficacy of anti-CTLA-4 therapy against melanoma. J Exp Med. 2013; 210:1695–1710. [PubMed: 23897981]

63. Stritesky GL, Xing Y, Erickson JR, Kalekar LA, Wang X, Mueller DL, Jameson SC, Hogquist KA. Murine thymic selection quantified using a unique method to capture deleted T cells. Proceedings of the National Academy of Sciences of the United States of America. 2013; 110:4679–4684. [PubMed: 23487759]

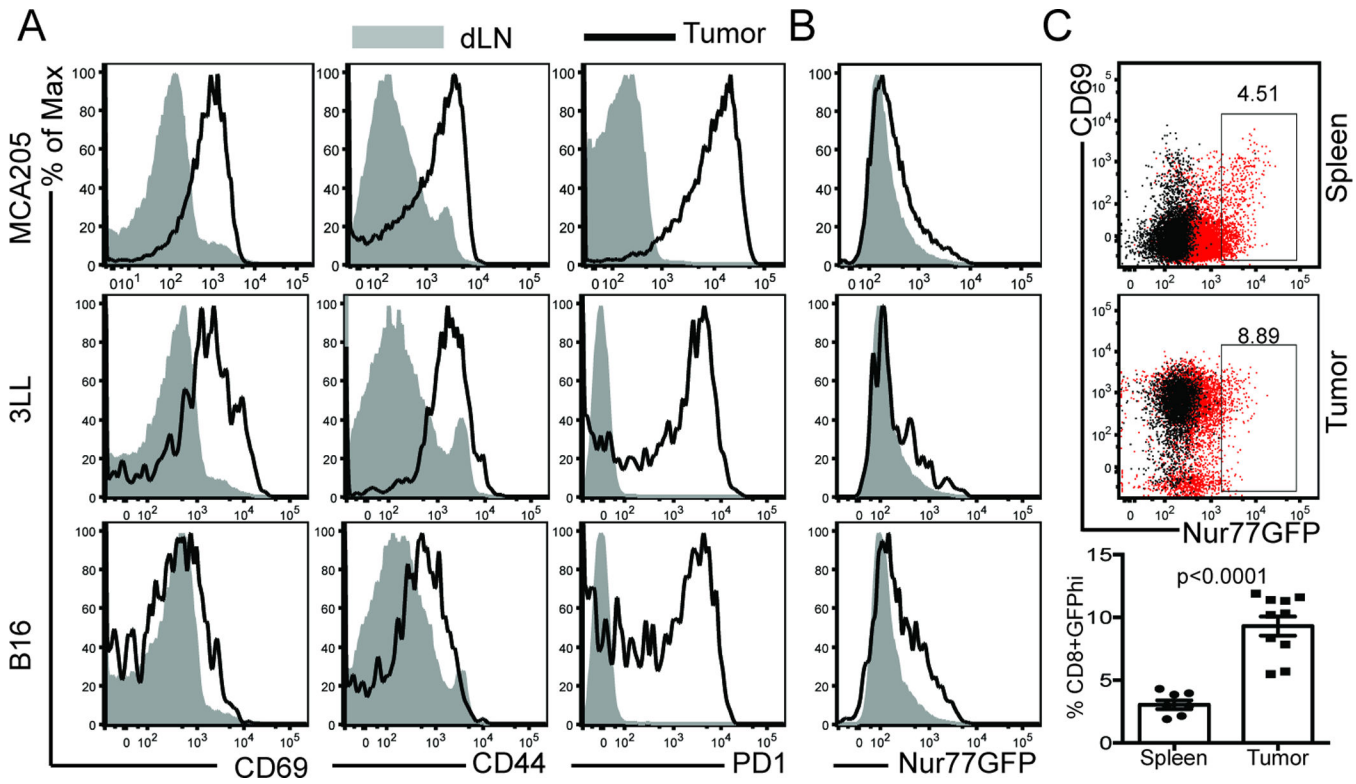

Figure 1. T cell activation markers within the tumor

A) Traditional markers of T cell activation were assessed on T cells from 3 different tumor models and paired draining lymph nodes 10–14 days after tumor inoculation on the hind flank. B) Nur77GFP expression on these same CD8 T cells was compared to activation molecule expression. C) Frequency of GFPhi CD8 T cells in spleen (top) versus tumor (bottom) of MCA205 tumor bearing mice. Data are representative of more than 6 experiments with n=3 animals per tumor model per experiment. Unpaired two-tailed Student's *t* test was used for statistical analysis and mean with SEM is shown.

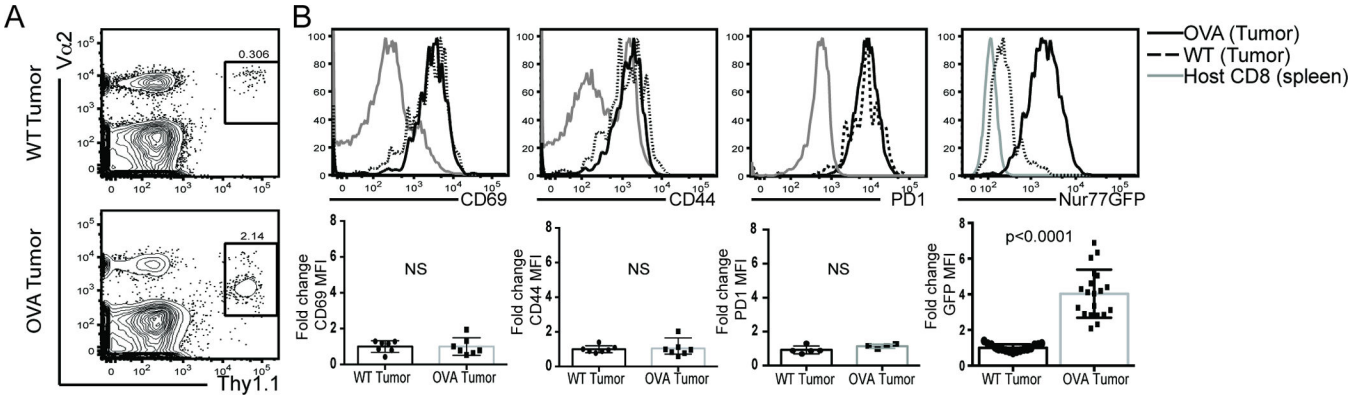

Figure 2. Tumor antigen specific upregulation of GFP

OVA tolerant POET mice were inoculated on the hind flanks with either MCA205 (WT) tumor cells or MCA205-OVA (OVA) expressing tumors. Ten days after tumor inoculation, OT-I/Thy1.1/Nur77GFP splenocytes were adoptively transferred into tumor bearing animals. A) Five days post adoptive transfer, OT-I T cells (identified by expression of Thy1.1 and their TCR alpha chain, Vα2) were isolated from the tumors. B) T cell activation markers were assessed on OT-I versus endogenous polyclonal CD8 T cells from WT (black dotted line, circles in bar graph) or OVA-expressing tumors (solid black line, squares in bar graph). Fold change was calculated from MFI of each activation marker on OTI T cells isolated from OVA expressing or WT tumors. Data are representative of 6 experiments with n=3–5 animals per treatment group per experiment. Unpaired two-tailed Student's *t* test was used for statistical analysis and data represents mean with SD.

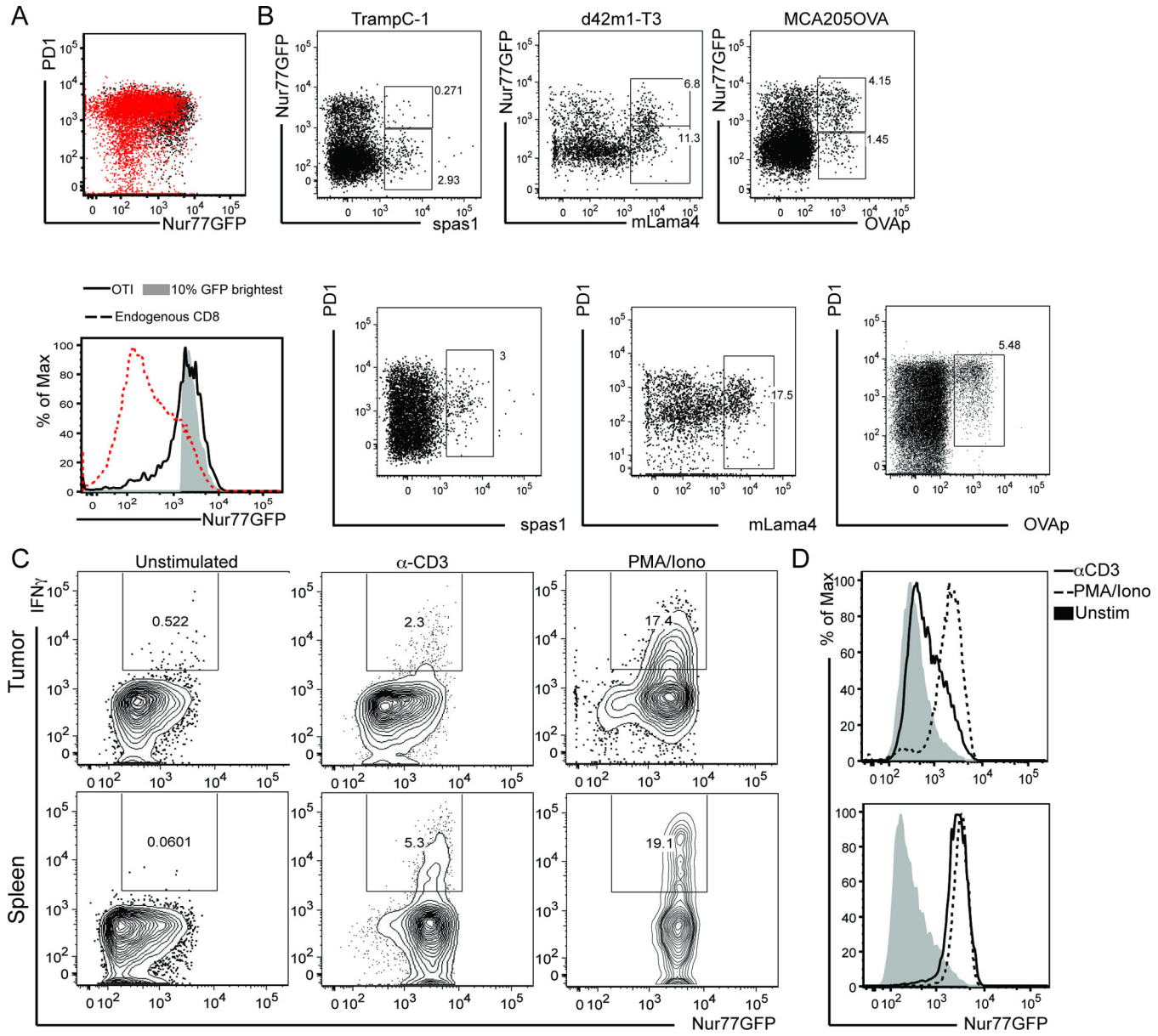

Figure 3. Tumor infiltrating CD8 T cells receive strong TCR signals

Nur77GFP mice were inoculated with A) MCA205-OVA expressing tumor cells on the hind flank. Once tumors were ~75mm^2, 10^6 OT-I/Thy1.1/Nur77GFP T cells were adoptively transferred (AT). Six days after AT, OT-I T cells were recovered from the tumor and OT-I/GFP expression (black dot plot/solid black line) was compared to the total population of endogenous CD8+ T cells (dotted line) as well as to the brightest GFP+ CD8+ T cells (shaded histogram). Gated on live/TCRβ+/CD8+ for endogenous and live/TCRβ+/CD8+/Thy1.1+ for OT-I histograms. B) Animals were inoculated with TRAMPC-1, d42m1-T3, or MCA205OVA tumor cells in 100μL Matrigel on the hind flank. 5–7 days after inoculation, tumors were harvested and tumor antigen specific T cells identified by MHC I tetramers for known tumor antigens. GFP and PD1 expression was evaluated. C) At ~d14 after MCA205 tumor inoculation in Nur77GFP mice, bulk digested tumor (top) or splenocytes (bottom)

were stimulated with anti-CD3 or PMA/Ionomycin for 4 hours before performing intracellular cytokine staining for IFNγ. D) Nur77GFP expression after stimulation in tumor vs spleen. Data shown is representative of 3 experiments with n=4 mice per experiment.

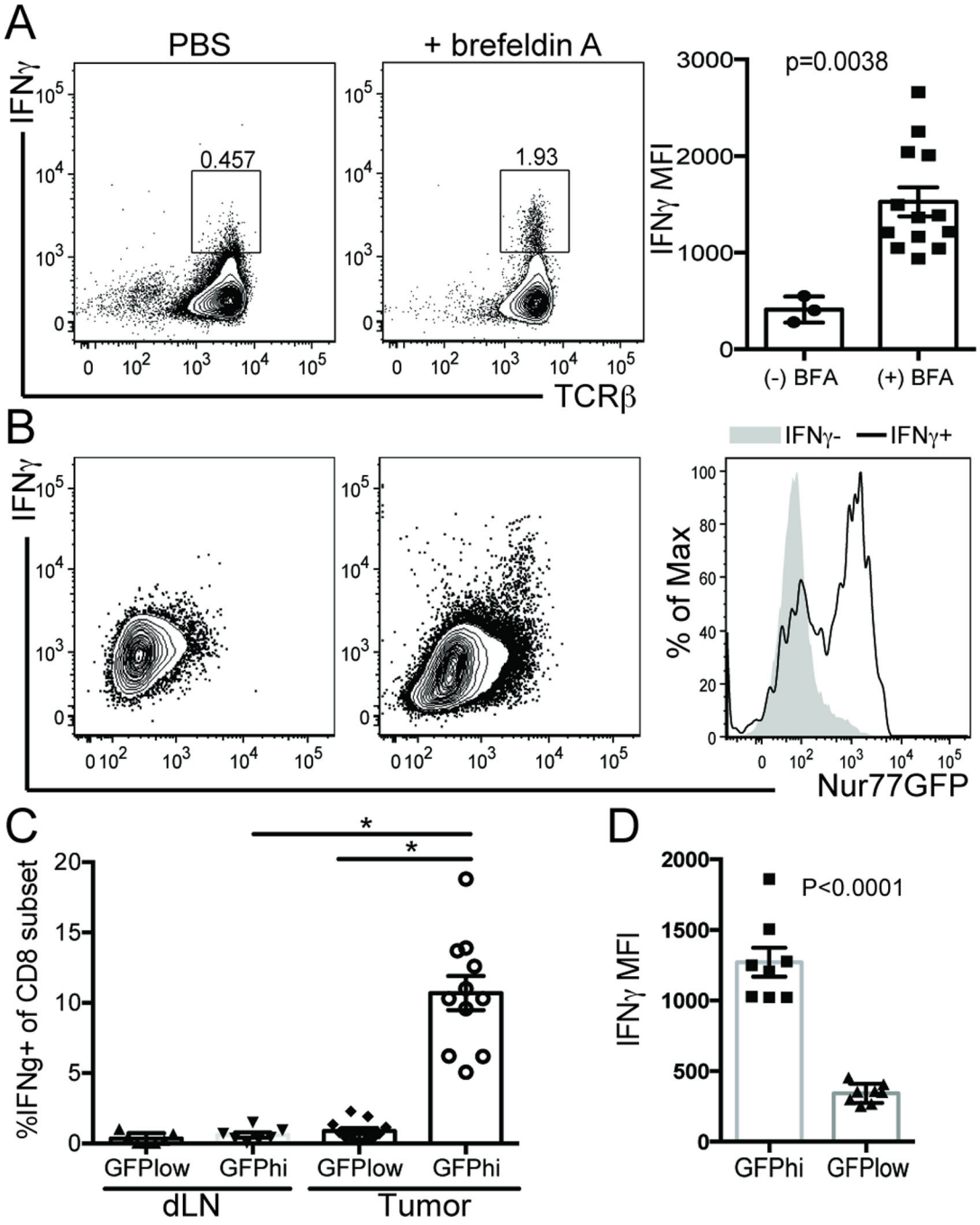

Figure 4. Nur77GFPhi CD8+ tumor infiltrating T cells make IFNγ

Nur77GFP mice were inoculated with MCA205 tumor cells on the hind flanks. ~12 days after tumor inoculation *in situ* IFNγ was assessed 6 hours after animals were injected with Brefeldin A or PBS alone. A) IFNγ production by T cells in tumor draining lymph nodes and B) tumor. The histogram overlays are representative of GFP expression from IFNγ- (shaded grey) and IFNγ+ (black line) populations of CD8 T cells. C) Percentage of IFNγ producing CD8 T cells in GFPhi vs GFPlow T cell subsets from tumor and dLN. D) IFNγ MFI in TCRβ+CD8+Nur77GFP subsets from the tumor. Data are representative of 3

experiments with n=3 animals per treatment group. Unpaired two-tailed Student's *t* test was used for statistical analysis of two groups and graphed as mean with SEM. For more than two groups, a one-way ANOVA multiple comparisons analysis was used and *p≤0.0001.

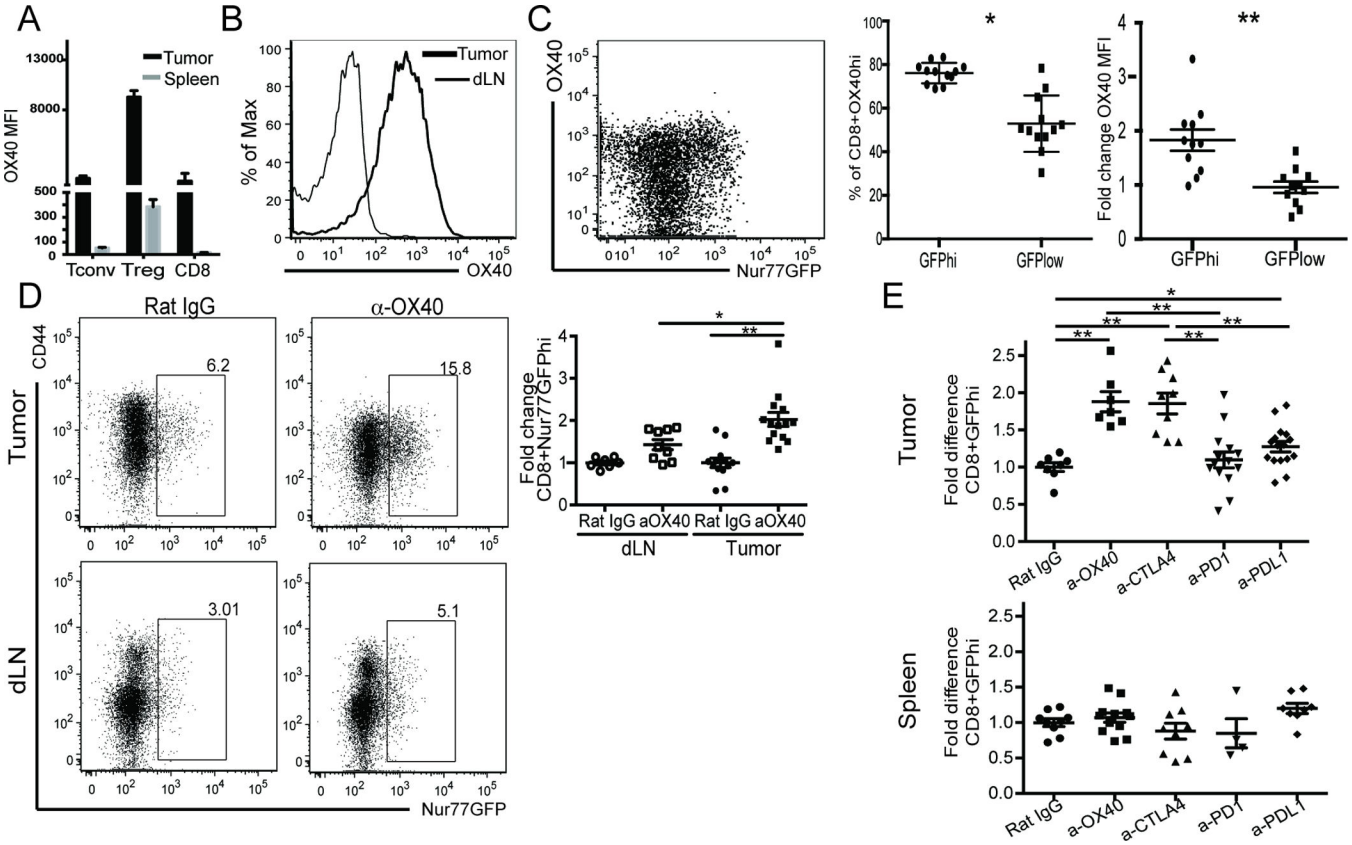

Figure 5. OX40 immunotherapy expands high affinity CD8 T cells

A) CD4+Foxp3- (Tconv), CD4+Foxp3+ (Treg), and CD8 T cells from tumor and spleen of Foxp3RFP MCA205 tumor-bearing animals were isolated and OX40 MFI evaluated via flow cytometry. Gated on live/TCRβ+/. B) Expression of OX40 on CD8 T cells from the tumor (bold histogram) and spleen (thin histogram) of MCA205 tumor bearing animals. C) Expression of OX40 in Nur77GFP CD8+TIL. The bar graph shows the frequency of OX40+CD8+ within GFP subsets (left) and fold change in OX40 expression of CD8+GFPhi TIL to CD8+GFPlow subset of TIL (right) isolated from MCA205 bearing Nur77GFP mice. D) Nur77GFP MCA205 bearing animals were treated with 2 × 250μg αOX40 or rat IgG control when tumors were ~80mm^2 in size. 7d after initiating treatment, TIL were isolated and fold increase in GFPhi T cells over rat IgG was determined. GFPhi gates were determined from a C57BL/6 control **p≤0.05, **p≤0.0001. E) MCA205 tumor bearing GFP mice were treated at day 10 post tumor inoculation with 2 × 250μg rat IgG, α-OX40, or α-CTLA4, or 3 × 200μg α-PD1 or α-PD-L1. All animals were harvested day 7 after therapy was started. Fold change in frequency of GFPhi CD8 T cells as compared to rat IgG control in tumor vs spleen. Data are representative of A-B) 3 experiments, n=4, C) more than 6 experiments n=3, D-E) 3 experiments n=3/group. For two-population comparison, student's t-test was used and graphed as mean with SEM. Multiple populations were analyzed using one way multiple comparisons ANOVA *p≤0.01, ** p≤0.0001.

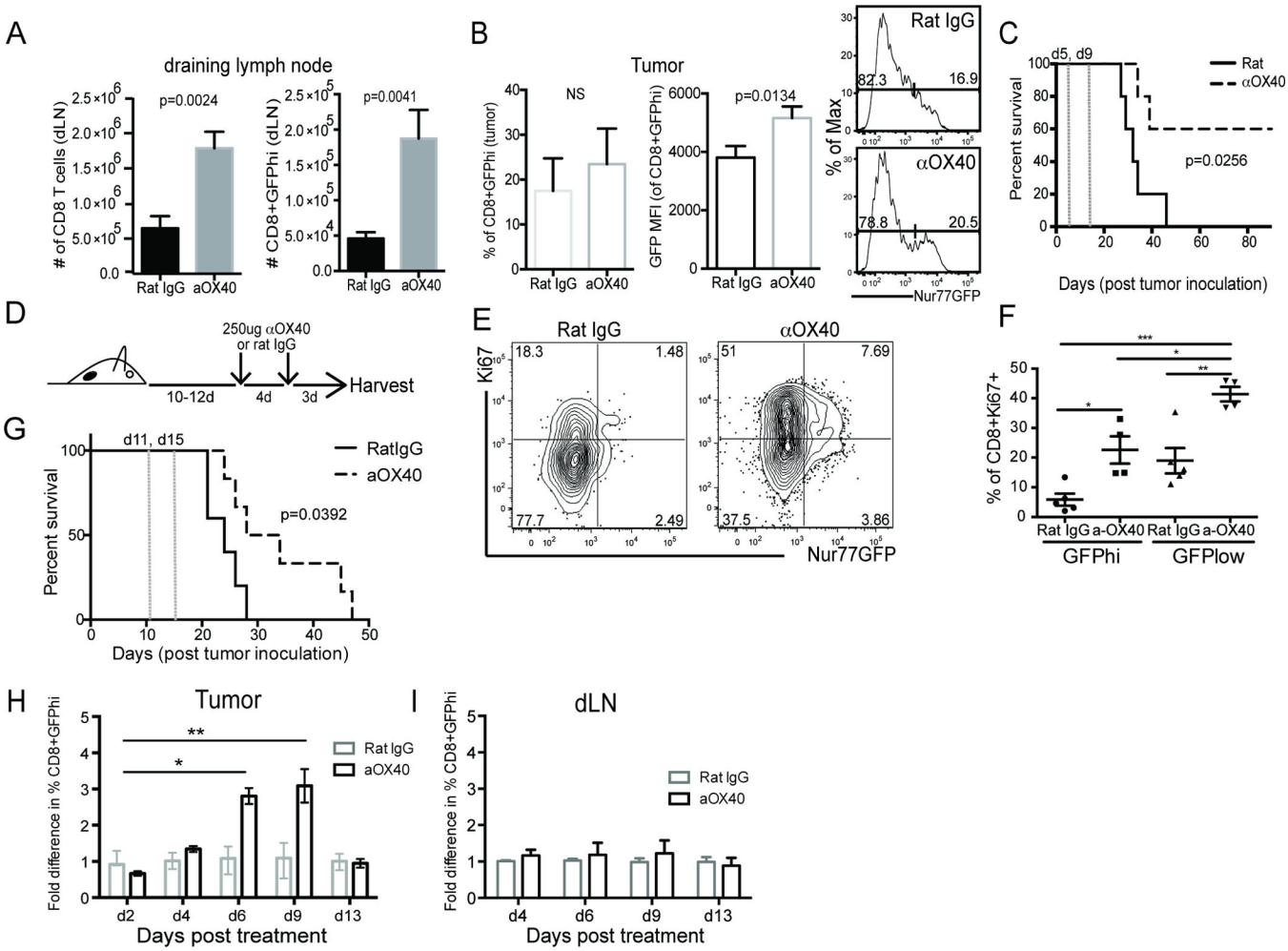

Figure 6. Expansion of GFPhi TIL after anti-OX40 immunotherapy enhances anti-tumor immunity

A-B) Nur77GFP MCA205 tumor-bearing mice were treated on days 5 and 9 after tumor inoculation with 2 doses of 250μg α−OX40 or control rat IgG. On day 10, one cohort of animals was euthanized and tumor and draining lymph nodes (dLN) were harvested, counted, and stained for flow cytometry analysis of GFP expression. C) The second cohort was monitored for long-term survival. Dotted vertical lines represent when animals were treated with immunotherapy. Data is representative of at least 2 independent experiments. D) Experimental design for E-G. E-F) Day 7 after 2 × 250μg of α-OX40 or rat IgG animals were euthanized, tumors harvested, cells fixed and intracellular staining performed for proliferation analysis. Data are representative of mean percentage of CD8+Ki67+ cells from each of 4 independent experiments. One way multiple comparison ANOVA was used for statistical analysis with * p≤0.05, **p≤0.01, ***p≤0.0001. G) Survival of rat IgG (solid line) and αOX40 treated (dotted line) MCA205 tumor bearing animals treated according to the experimental design in D). Dotted vertical lines represent when animals were treated with immunotherapy. Log Rank (Mantel Cox) test was used for statistical analysis. H) Fold change of percent GFPhi CD8 T cells in the tumor or I) draining LN (dLN) after a single dose of α-OX40 or rat IgG antibody given at day 10 after tumor inoculation. Median fold

change in %CD8+GFPhi T cells is graphed with SEM indicated. Data was compiled from 3 independent experiments in which GFPhi frequency for OX40 treated animals was determined by first gating through live/TCRβ+/CD8+/OX40dim T cells or through live/TCRβ+/CD8+ for rat IgG treated animals *p≤0.001, **p≤0.0001.

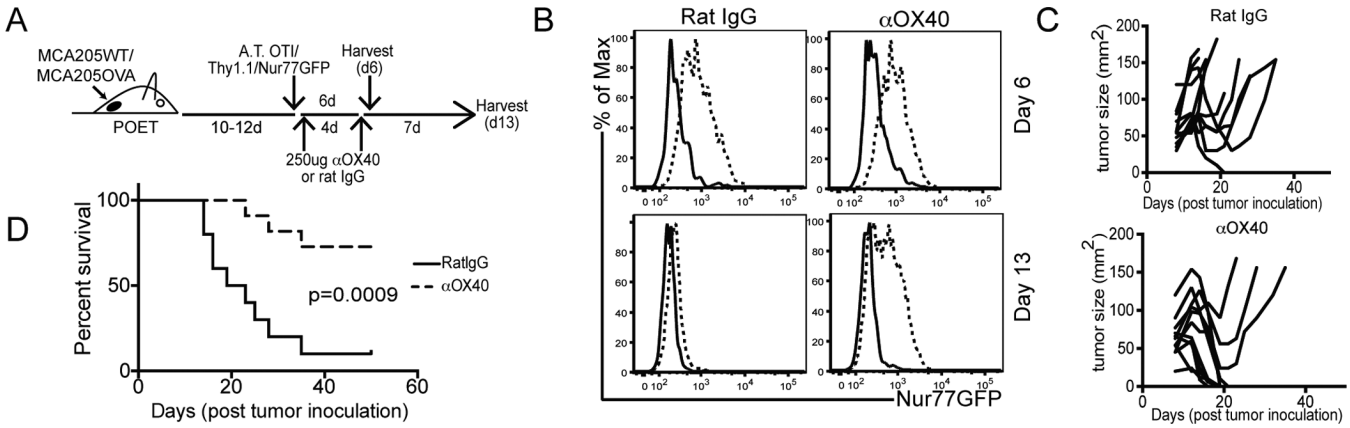

Figure 7. anti-OX40 immunotherapy maintains Nur77GFP induction on tumor antigen-specific T cells

OVA tolerant POET mice were inoculated on the hind flank with either MCA205 WT or MCA205 OVA tumors and treated according to the experimental design in A). The first cohort of animals was analyzed at B) day 6 (top row) after adoptive transfer and the second (bottom row) at day 13 after adoptive transfer. Expression of Nur77GFP is indicated on live/TCRβ+/CD8+/Thy1.1+ T cells from the tumor. An independent cohort of animals were treated according to A) and monitored for long-term survival. C) spider plots and D) survival curves are shown for these animals. Data are representative of 3 independent experiments with a minimum of n=5 animals per tumor model and treatment group.